



## Micro- and nanostructured electro-active polymer actuators as smart muscles for incontinence treatment

Bekim Osmani, Tino Töpper, Christian Deschenaux, Jiri Nohava, Florian M. Weiss, Vanessa Leung, and Bert Müller

Citation: [AIP Conference Proceedings](#) **1646**, 91 (2015); doi: 10.1063/1.4908588

View online: <http://dx.doi.org/10.1063/1.4908588>

View Table of Contents: <http://scitation.aip.org/content/aip/proceeding/aipcp/1646?ver=pdfcov>

Published by the [AIP Publishing](#)

---

### Articles you may be interested in

[Electro-active polymer transduction for distributed netted sensing](#)

J. Acoust. Soc. Am. **123**, 3013 (2008); 10.1121/1.2932614

[An active energy harvesting scheme with an electroactive polymer](#)

Appl. Phys. Lett. **91**, 132910 (2007); 10.1063/1.2793172

[Self-oscillating electroactive polymer actuator](#)

Appl. Phys. Lett. **90**, 184104 (2007); 10.1063/1.2735931

[An electroactive polymer-ceramic hybrid actuation system for enhanced electromechanical performance](#)

Appl. Phys. Lett. **85**, 1045 (2004); 10.1063/1.1779341

[Wrinkled polypyrrole electrode for electroactive polymer actuators](#)

J. Appl. Phys. **92**, 4631 (2002); 10.1063/1.1505674

---

# Micro- and Nanostructured Electro-Active Polymer Actuators as Smart Muscles for Incontinence Treatment

Bekim Osmani<sup>1, a</sup>, Tino Töpper<sup>1, b</sup>, Christian Deschenaux<sup>2, c</sup>, Jiri Nohava<sup>2, d</sup>, Florian M. Weiss<sup>1, e</sup>, Vanessa Leung<sup>1, f</sup>, and Bert Müller<sup>1, g</sup>

<sup>1</sup> *Biomaterials Science Center, University of Basel, c/o University Hospital, 4031 Basel, Switzerland*

<sup>2</sup> *Anton Paar TriTec SA, Rue de la Gare 4, Galileo Center, 2034 Peseux, Switzerland*

a) Corresponding author: bekim.osmani@unibas.ch

b) tino.toepper@unibas.ch, c) christian.deschenaux@anton-paar.com, d) jiri.nohava@anton-paar.com,

e) florian.weiss@unibas.ch, f) vanessa.leung@unibas.ch, g) bert.mueller@unibas.ch

**Abstract.** Treatments of severe incontinence are currently based on purely mechanical systems that generally result in revision after three to five years. Our goal is to develop a prototype acting in a natural-analogue manner as artificial muscle, which is based on electro-active polymers. Dielectric actuators have outstanding performances including millisecond response times, mechanical strains of more than 10 % and power to mass densities similar to natural muscles. They basically consist of polymer films sandwiched between two compliant electrodes. The incompressible but elastic polymer film transduces the electrical energy into mechanical work according to the Maxwell pressure. Available polymer films are micrometers thick and voltages as large as kV are necessary to obtain 10 % strain. For medical implants, polymer films should be nanometer thin to realize actuation below 48 V. The metallic electrodes have to be stretchable to follow the strain of 10 % and remain conductive. Recent results on the stress/strain behavior of anisotropic EAP-cantilevers have shown dependencies on metal electrode preparation. We have investigated tunable anisotropic micro- and nanostructures for metallic electrodes. They show a preferred actuation direction with improved stress-strain behavior. The bending of the cantilever has been characterized by the laser beam deflection method. The impact of the electrode on the effective Young's Modulus is measured using an Ultra Nanoindentation Tester with an integrated reference system for soft polymer surfaces. Once ten thousand layers of nanometer-thin EAP actuators are available, devices beyond the envisioned application will flood the market.

## INTRODUCTION

The treatment of severe fecal incontinence is a reasonable and growing market due to demographic changes in developed countries [1]. Current devices, usually consist of a pump with a liquid-filled inflating cuff, are slow and difficult to operate [2]. They improve incontinence but show considerable complication and revision rates [3].

We propose a device, which is based on dielectric electro-active polymers (EAP). These actuators can be designed to perform muscle-like actuations or imitate muscle functions.

Dielectric elastomer actuators (DEAs) are referred to artificial muscles because of the performance including millisecond response, mechanical strains of more than 10 %, and the power-to-mass densities similar to natural muscles [4, 5]. These actuators offer perspectives for bio-mimetic applications because of the large actuations [6] and sensing ability. Several examples are reported in robotics and haptic feedback devices [5]. However, key challenges like operation at low voltages, large-scale manufacturability and integrated sensing remain still unsolved to enable a breakthrough of this technology.

The working principle of a DEA is shown in Fig. 1. Here, the elastomer films are sandwiched between compliant electrodes.

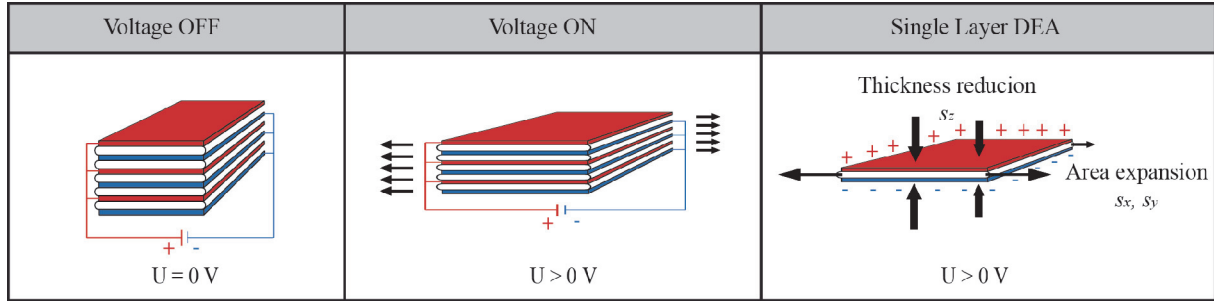


**FIGURE 1.** The sandwiched elastomer films respond to the electric field with a planar expansion.

Dielectric elastomer actuators transduce the applied voltage into mechanical work according to the Maxwell stress [7] often termed the actuation pressure  $p$ :

$$p = \varepsilon \cdot \varepsilon_0 \cdot E^2 = \varepsilon \cdot \varepsilon_0 \cdot \frac{U^2}{t_{ef}^2} \quad (1)$$

where  $\varepsilon$  is the dielectric constant of the elastomer,  $\varepsilon_0$  the vacuum permittivity,  $E$  the induced electric field,  $U$  the applied voltage and  $t_{ef}$  the thickness of the elastomer film. The compressive strain  $s_z$  can be written as:

$$s_z = -\frac{\Delta t_{ef}}{t_{ef}} = -\varepsilon \cdot \varepsilon_0 \cdot \frac{U^2}{Y \cdot t_{ef}^2} = -\frac{p}{Y} \quad (2)$$

Assuming that the elastomer is incompressible, with a bulk compressibility much higher than its elastic modulus  $Y$  and with a Poisson ratio of 0.5, we can write for the planar strains  $s_x$  and  $s_y$ :

$$s_{x,y} = -0.5 \cdot s_z = \varepsilon \cdot \varepsilon_0 \cdot \frac{U^2}{2 \cdot Y \cdot t_{ef}^2} \quad (3)$$

For applications in medical implants we target driving voltages below 48 V. One would expect from the Eq. 3 that the planar strain for low voltages  $U$  can be achieved by simply reducing the elastomer film thickness  $t_{ef}$ . This is not the case since for thin layers, it is necessary to use the effective Young's modulus  $Y_{eff}$  of the stacked structure (electrode/ elastomer). For the uniform strain, Voigt [8] proposed the following model for sandwich materials:

$$Y_{eff} = Y_{ef} h_{ef} + Y_e h_e \quad (4)$$

where  $h_{ef}$  is the normalized elastomer thickness and  $h_e$  the normalized electrode thickness, with  $h_e + h_{ef} = 1$ . For the uniform stress state, Reuss [9] introduced this expression for a two-phase material:

$$Y_{eff} = \frac{Y_{ef} \cdot Y_e}{Y_{ef} h_e + Y_e h_{ef}} \quad (5)$$

Neither assumption is correct. For the Voigt model one would need two materials with the same Poisson ratio and for Reuss the interface between the two phases is not considered. Since these estimations are good as upper and lower bounds, the actual value is often taken as the average of the two [10], known also as the Voigt-Reuss-Hill average:

$$Y_{VRH} = \frac{1}{2} \cdot \left[ \frac{Y_{ef} \cdot Y_e}{Y_{ef} h_e + Y_e h_{ef}} + (Y_{ef} h_{ef} + Y_e h_e) \right] \quad (6)$$

The elastomer thickness can be scaled down to some hundred nanometers but there are restrictions for the electrode. A minimal thickness for a conductivity of  $< 10 \Omega/\text{square}$  is needed to ensure a reaction time below 500 ms of the actuator. This leads to an increase of the electrode-to-elastomer ratio and therefore to an increase of the  $Y_{VRH}$  as shown in Fig. 2, especially for rigid electrodes.

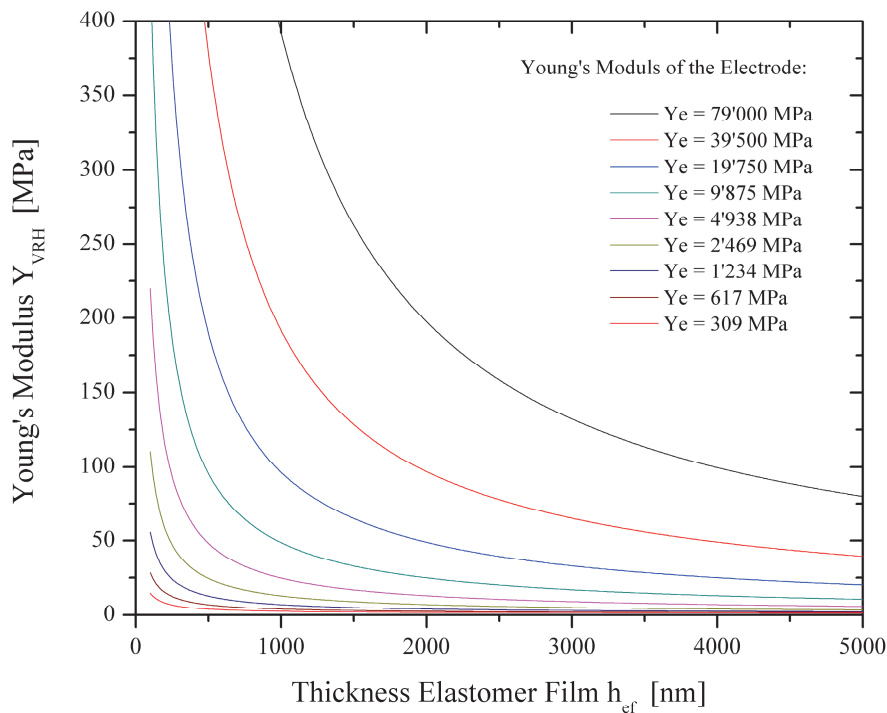


**FIGURE 2.** Plot for the Voigt-Reuss-Hill average as function of the elastomer thickness with a Young's Modulus  $Y_{ef} = 1 \text{ MPa}$  for selected moduli  $Y_e$  of electrode with  $h_e = 10 \text{ nm}$ .

For medical applications, DEAs should work at voltages as low as 6 to 48 V and elastomer thicknesses below 1000 nm to ensure actuation strains larger than 10%. To avoid a dominating stiffness of the electrode with respect to the elastomer films, the fabrication of highly stretchable or non-rigid electrodes is inevitable [10, 11].

We have investigated DEA cantilevers with planar and wrinkled electrodes using a custom-built cantilever beam bending apparatus. The electrodes were sputtered on a tunable wrinkled elastomer surface. It has been shown that uniaxial pre-stretched elastomer substrates form parallel wrinkles on the top due to the compressive strain between the deposited stiff film and the underlying soft substrate [12, 13]. The periodicity and amplitude of the wrinkled structures can be predicted for known film coatings and film thicknesses [13].

## MATERIAL AND METHODS

### Measurement of the Effective Young's Modulus

The effective Young's modulus of a single-layer dielectric actuator with an Au electrode was measured using an UNHT - Ultra Nano Indentation Tester (Anton Paar TriTec SA, Switzerland). The UNHT works with an integrated reference system, which can be placed on the rigid sample holder to prevent a possible sinking of the reference system into the soft elastomer film [14]. When the reference tip touches the surface, an indenter tip with a known geometry moves into the sample to be tested, applying an increasing normal load. The position of the indenter relative to the sample surface is monitored with a differential capacitive sensor (Fig. 3).

Two samples were cut and fixed on an adjustable holder. On the first sample, a 5  $\mu\text{m}$ -thin polydimethylsiloxane (PDMS) film (Elastosil 745 A/B, Wacker Chemie AG, Munich, Germany) was spin-coated on a 3-inch Si wafer (Si-Mat Silicon Materials, thickness  $381 \pm 25 \mu\text{m}$ ) and thermally cross-linked at a temperature of 80  $^{\circ}\text{C}$  for a period of 24 h. On the second sample, an additional electrode of 10 nm Au was magnetron sputtered (BALZERS UNION SCD 040 SYSTEM, Balzers, Lichtenstein). The edge of the sample holder was used as a fixed reference. The indenter with parameters given in the table of Fig. 3 was approaching the surface at a speed of 33 nm/s. At the maximum load of 15  $\mu\text{N}$ , the indenter maintained this value for a period of 30 s to measure the creep into the elastomer. The power law method by Oliver & Pharr [14] was used to determine the hardness and elastic modulus of the material.

UNHT Parameters:	Schematic of the UNHT head (patented design)
Indenter Type:	Spherico-Conical (SE-A19)
End-Radius:	20 $\mu\text{m}$
Cone Angle:	90 $^{\circ}$
Approach/Retract Speed:	2000 nm/min
Approach Distance:	4000 nm
$F_N$ Contact:	7 $\mu\text{N}$
Loading/Unloading:	linear
Loading rate:	30 $\mu\text{N}/\text{min}$
Maximum Load:	15 $\mu\text{N}$
Holding time at max. load:	30 s
Reference contact load:	200 $\mu\text{N}$ (on substrate)

A0: motorized z-table

**FIGURE 3.** The parameters for the nano indentation tests are shown on the left. The schematic on the right gives an overview of the UNHT head with the indenter force  $F_N$ , the load cell capacitive sensors C1, C2, the penetration depth differential capacitive sensor C3 and the cell springs K1 and K2.

The displacement resolution was 0.0004 nm (noise floor of 0.03 nm) with a normal force resolution of 0.001  $\mu\text{N}$  (noise floor of 0.1  $\mu\text{N}$ ).

## Preparation of the DEA Cantilevers

The anisotropic cantilevers structures were prepared according to the steps shown in Fig. 4. Polyetheretherketone (PEEK) substrates (APTIV 2000, Victrex, Lancashire, UK) with a thickness of 25  $\mu\text{m}$  were cut to the size of 3-inch wafers and cleaned with acetone (Merck KGaA, Darmstadt, Germany). Au (Lesker, East Sussex, United Kingdom) was sputtered (Balzers Union SCD 040 System, Balzers, Liechstenstein) on both sides of the PEEK film, 50 nm on the reflective side and 25 nm on the side of the actuator. The thickness was measured using a quartz crystal microbalance (QSG 301, Balzers, Liechtenstein).

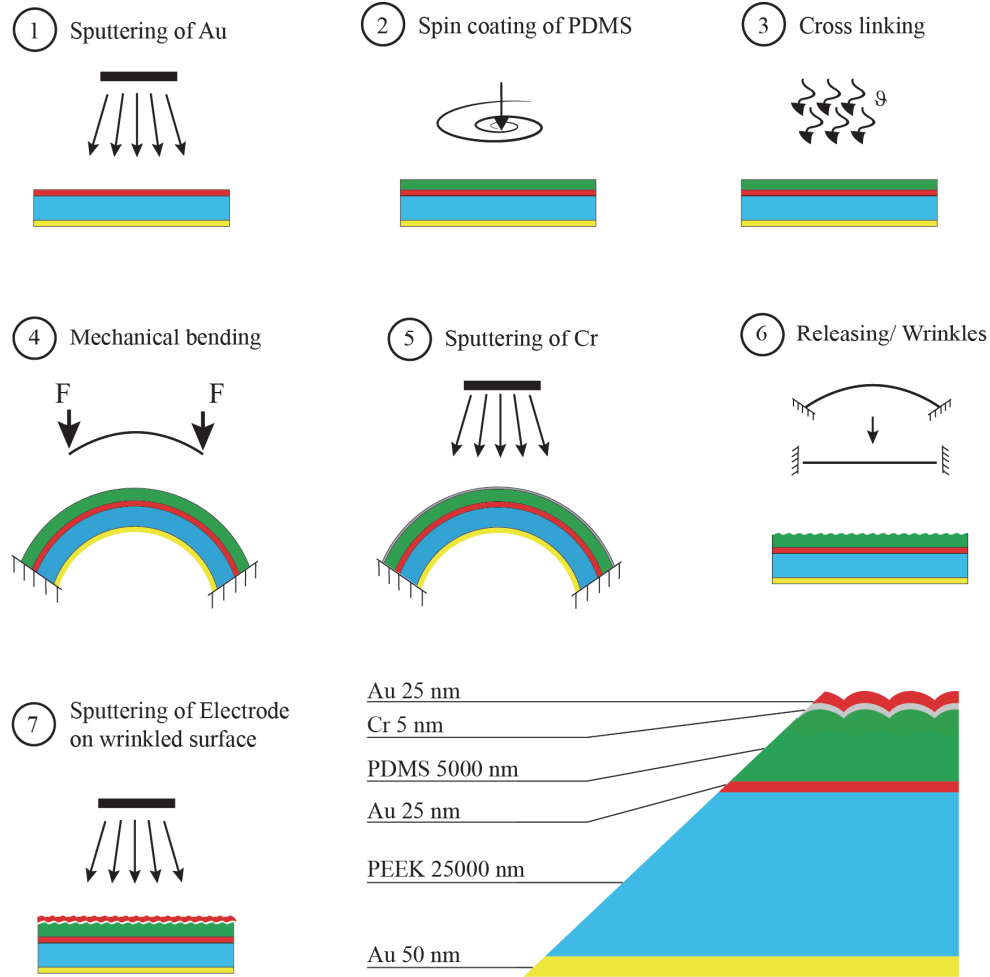


**FIGURE 4.** Preparation of the actuator with wrinkled electrode on the cantilever.

PDMS was mixed in a volume ratio 1:1 of component A and B and spin-coated at a rotational speed of 2000 rpm for 2 minutes, resulting in a film thickness of 5  $\mu\text{m}$ . For a better access to the electrode, the substrate end (about 5 mm) was dip washed into ethyl acetate (Fisher Scientific, Reinach, Switzerland) to dissolve and wash off the PDMS. The remaining PDMS was thermally cross-linked at a temperature of 80  $^{\circ}\text{C}$  for a period of 24 hours.

The sample was mechanically bended to introduce a tensile strain on the PDMS film, where approximately 5 nm of Cr (Lesker, East Sussex, UK) were sputtered. After releasing, wrinkles appeared because of the inability of the Cr-film to follow the compressive strain on the PDMS [15, 16]. Finally, the conductive Au electrode was sputtered on the wrinkled surface. For reference measurements, we used a shadow mask to cover half of the 3 inch-wafer during the deposition of Cr and fabricated reference cantilevers with an Au electrode 25 nm thin.

## Cantilever Bending Apparatus

Rectangular cantilevers with dimensions of 4 mm × 14 mm were cut out of the 3-inch wafer and fixed on a polytetrafluoroethylene (PTFE) holder. Both electrodes were contacted with flexible spring tips and connected to the power supply (Stanford Research System PS310, GMP SA, Lausanne, Switzerland). The cantilever holder was mounted inside a floatable and thermally decoupled chamber. The cantilever was hanging vertically to avoid a possible bending caused by the gravity.

The laser beam (Stream Line Laser System L2S-SL-660-1-S-A, Laser 2000, Germany) illustrated in Fig. 5 was adjusted to be reflected at a distance of 2 mm from the bottom of the Cantilever. The reflected laser beam hit the position sensitive photo detector (DUM-SpotOn Compact PSD Detector, Laser 2000, Germany) in the center. The PSD detector was mounted on an x-y-z-table and recorded the deflection of the laser beam during the actuation cycles. Voltage ramps were applied stepwise from 6 to 48 V. Cantilevers for the reference measurements were cut from the other half of the wafer without the wrinkled electrode on the top.

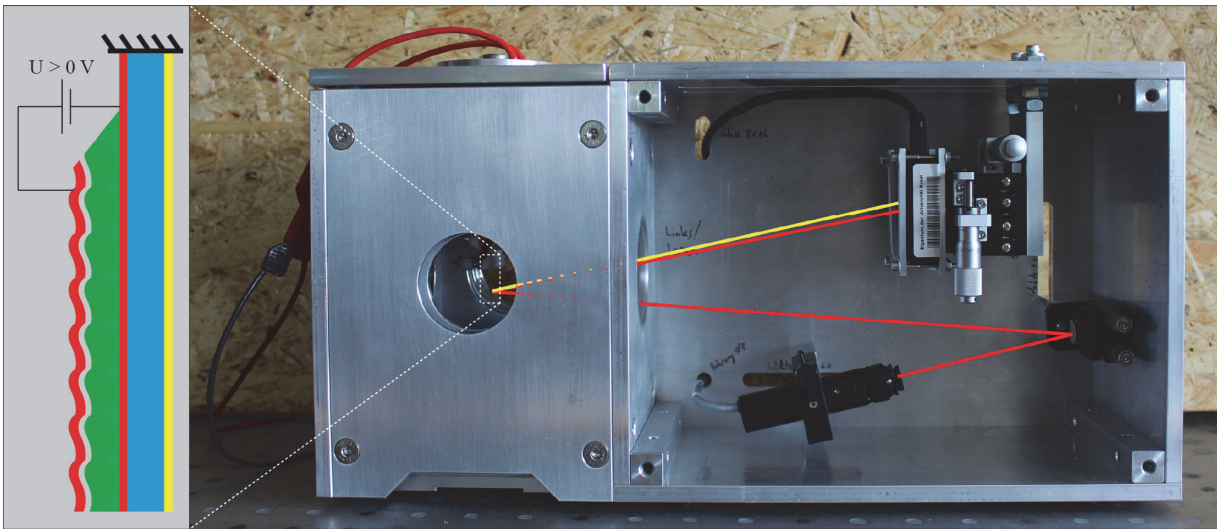


**FIGURE 5.** The custom-built apparatus is used for the characterization of mechanical properties of anisotropic EAP structures on PEEK cantilevers. The deflection of the laser beam is measured using a position sensitive photo detector.

## RESULTS

### Characterization of the Effective Young's Modulus

The average hardness  $H_{IT}$  shown in Table 1 is  $0.128 \pm 0.001$  MPa for the single PDMS film and  $0.235 \pm 0.008$  MPa for the PDMS + 10 nm Au electrode. The hardness  $H_{IT}$  is calculated from the measured maximum load  $F_{\max}$  of the indenter head divided by the projected contact area  $A_{p,hc}$  at the contact depth  $h_c$ :

$$H_{IT} = \frac{F_{\max}}{A_{p,hc}} \quad (7)$$

The Young's modulus of the sample  $Y_s$  (Eq. 8) is defined as a function of the reduced modulus and the modulus of the indenter  $Y_i$ . The reduced modulus  $Y_r$  of the indentation contact is a function of the contact stiffness (derivative at the peak load) and projected contact area  $A_{p,hc}$ . Since Oliver and Pharr's method does not consider any time effects, a creep analysis was performed to get additional information regarding the viscous behavior of the samples.

$$\frac{1}{Y_r} = \frac{1-\nu_i^2}{Y_i} + \frac{1-\nu_s^2}{Y_s} \quad (8)$$

Fig. 6 shows selected indentation curves for both samples. The maximum penetration depths for the PDMS + 10 nm Au electrode were 849 nm and 881 nm, while for the PDMS films they were 1870 nm and 1927 nm. During the holding time of 30 s, the creeps for the PDMS + 10 nm Au electrode were approximately 11 nm and 6 nm, while for the PDMS films the measured creeps were 71 nm and 85 nm.

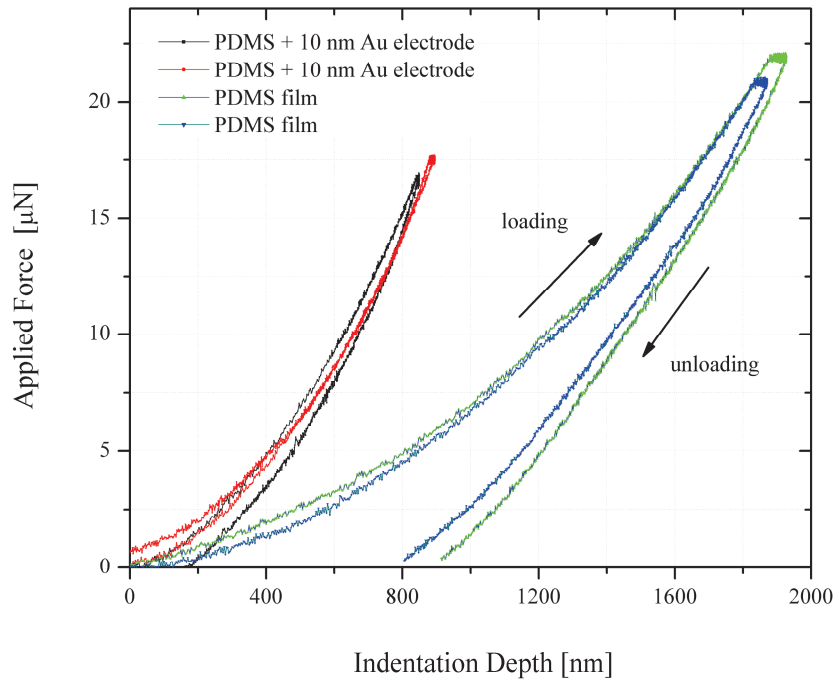


**FIGURE 6.** Indentation curves for PDMS film and PDMS + 10 nm Au electrode.

Comparing the results from Table 1 with the plots in Fig. 2 and Eq. 6, one can assume a Young's modulus of 3'000 MPa for the 10 nm Au electrode.

**TABLE 1.** Calculation of hardness  $H_{IT}$ , and the Young's modulus  $Y_s$  with and without creep.

Indentation		PDMS film [MPa]	PDMS + 10 nm Au electrode [MPa]
$H_{IT}$ (O&P)	Sample 1	0.129	0.227
	Sample 2	0.127	0.243
	<b>Mean</b>	<b>0.128 ± 0.001</b>	<b>0.235 ± 0.008</b>
$Y_s$ (O&P)	Sample 1	1.683	4.051
	Sample 2	1.691	3.861
	<b>Mean</b>	<b>1.687 ± 0.004</b>	<b>3.956 ± 0.095</b>
$Y_s$ (Creep)	Sample 1	0.976	2.701
	Sample 2	1.015	2.623
	<b>Mean</b>	<b>0.996 ± 0.02</b>	<b>2.662 ± 0.039</b>

## Actuator Performance

The cantilevers with wrinkled electrodes are shown in Fig. 7. The wrinkles have a periodicity of about  $5.5 \mu\text{m}$  and an amplitude of  $650 \text{ nm}$ .

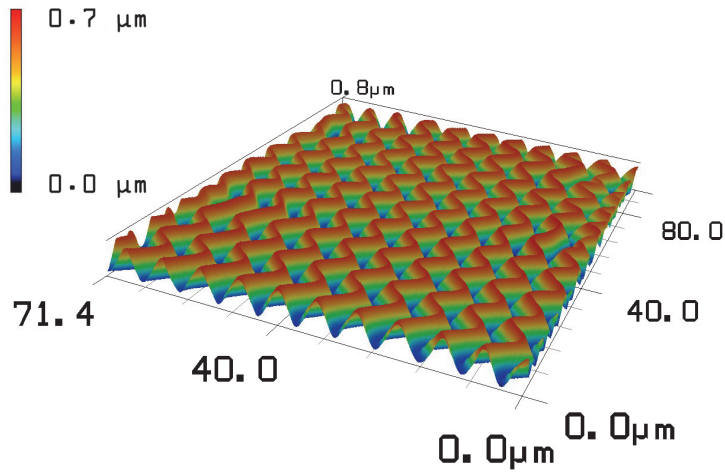


**FIGURE 7.** Scan with a 3D optical microscope from Keyence of a DEA cantilever with oriented wrinkles.

Measurements for voltage ramps of up to  $48 \text{ V}$  are shown in Fig. 8. The displacement on the PSD was for samples with wrinkled electrodes on average  $65\%$  larger than for the ones with planar electrodes. The fits for deflection curves are parabolic functions since the tensile strain  $s_x$  shown in Eq. 2, is also a function of  $U^2$ .

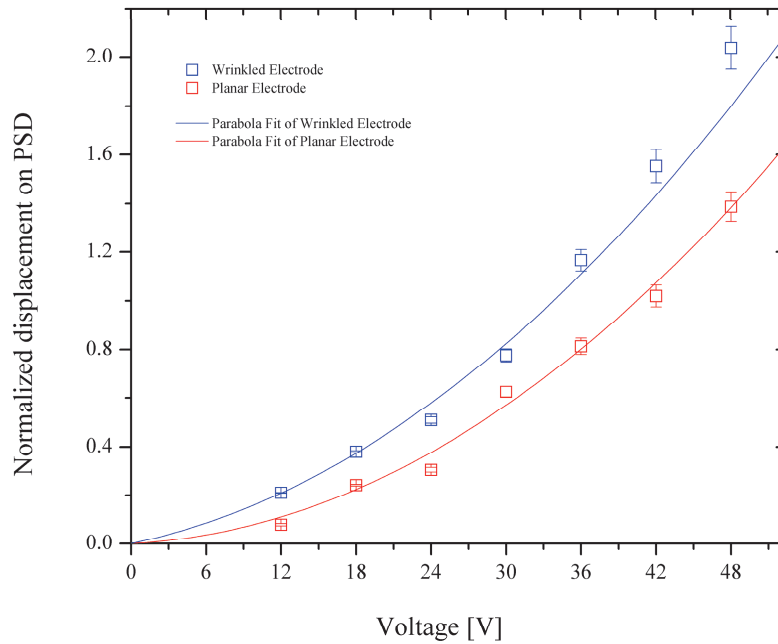


**FIGURE 8.** Analysis of the measured deflection.

Fig. 9 shows selected charging cycles for actuators with wrinkled and planar electrodes. The displacement of the reflected laser beam on the PSD was measured as a function of time for the maximum voltage of 350 V. Beside the reduced deflection seen in Fig. 8, one can measure a drift of 15 % for the actuator with planar electrodes within the time frame from 500 and 3800 ms. Actuators with wrinkled electrodes show a drift of about 2 %, maintaining the actuation within the oscillation peaks.

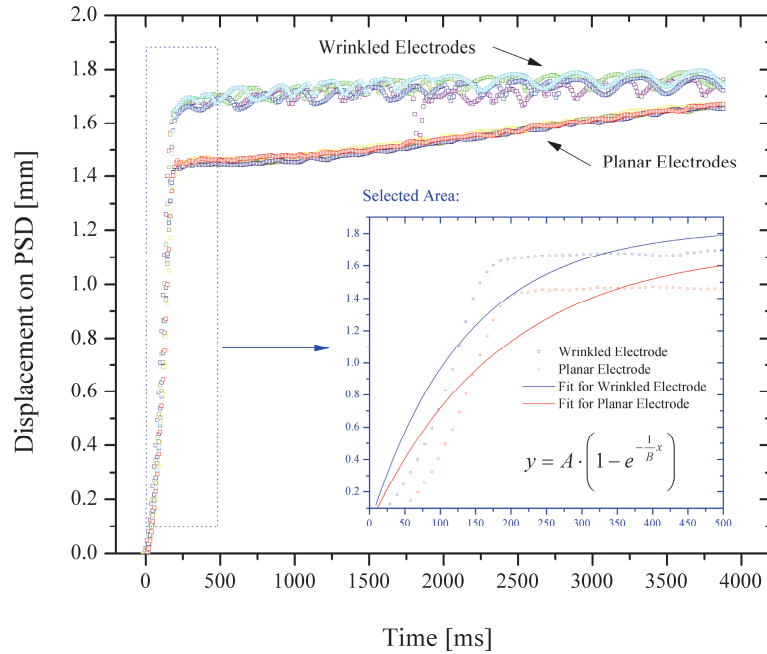


**FIGURE 9.** Charging curves of DEA Cantilevers.

As a simple model, DEAs can be considered as plate capacitors of two electrical conductors separated by a dielectric material. The fits of the charging curves in selected area (blue box) in Fig. 9 may be described by the charging behavior of a capacitor with a time constant  $\tau=R*C$ :

$$Q(t) = Q_0 \cdot \left( 1 - e^{-\frac{t}{RC}} \right) \quad (9)$$

From the fits, the calculated time constant for the wrinkled electrode was found to correspond to  $\tau = (134 \pm 12)$  ms and for the planar electrode  $\tau = (184 \pm 22)$  ms.

## DISCUSSION AND CONCLUSIONS

The stiffness and stretchability of conventionally fabricated actuators is dominated by planar metallic electrodes. We have shown that the stiffness of a single-layer actuator can successfully be measured using an Ultra Nano Indentation Tester. The penetration depth in pure PDMS was clearly larger than in the sample with an additional Au electrode. Measurements with the reference system on the PDMS were difficult because of the slightly sinking ball into the PDMS, even if the contact force was  $\leq 200 \mu\text{N}$  (the penetration depth is measured relative to the height reference). The assumed Young's modulus of about 3 GPa for the 10 nm Au electrode can be a result of the cracks and also islands of the sputtered Au on the elastomer film. One has to perform further measurements for elastomer films between 100 and 1000 nm to verify the chosen model.

We have demonstrated that actuators with wrinkled electrodes show a larger actuation and an improved stress-strain behavior. We expect to adjust the wavelength and amplitude of the wrinkles by deposition of different film coatings on the elastomer surface Eq. 10 [13] and thereby to fabricate actuators for larger strains:

$$\lambda = 2 \cdot \pi \cdot h_e \cdot \left[ \frac{(1 - \nu_{el}^2) \cdot Y_e}{3 \cdot (1 - \nu_e^2) \cdot Y_{el}} \right]^{\frac{1}{3}} \quad (10)$$

The drift in the deflection for actuators with planar electrodes in Fig. 9 can be a result of arising cracks in the Au electrode. The cracks could make it more stretchable and allow thereby a larger strain. For the wrinkled electrodes, we assume that the seen overlapped oscillations may be simple harmonic motions with a possible relation to the wavelength and the amplitude of the wrinkles.

The response time of the actuator with wrinkled electrodes seems to be faster than for the one without wrinkles. We can see from the fitted curves in Fig. 9 that the time constant  $\tau$  for the wrinkled electrode is about 27 % smaller. The initial part of the actuation from 0 to 150 ms does not correspond well to the exponential fit. This could be due to inertia or other mechanical effects of the anisotropic cantilever.

## ACKNOWLEDGMENTS

The authors gratefully acknowledge the funding of the Swiss National Science Foundation and the nano-tera.ch initiative (SmartSphincter). We thank Dr. Monica Schönenberger from the Nanotech Service Lab, Swiss Nanoscience Institute (SNI), Sascha Martin from the Mechanics Shop, Department of Physics, University of Basel and Victrex Europe for providing us with PEEK Cantilevers.

## REFERENCES

1. C. W. McGrother, "Epidemiology of Urinary Incontinence," in *Urinary and Fecal Incontinence*, edited by H. D. Becker, A. Stenzl, D. Wallwiener and T. T. Zittel, (Springer-Verlag, Berlin Heidelberg, 2005), pp. 13-23.
2. K. D. Hong, G. Dasilva, S. N. Kalaskar, Y. Chong and S. D. Wexner, *Journal of the American College of Surgeons* 217 (4), 718-725 (2013).
3. M. Goos, U. Baumgartner, M. Löhnert, O. Thomusch and G. Ruf, *BMC Surgery* 13, p. 45 (2013).
4. S. Ashley, *Scientific American* 10, 52-59 (2003).
5. I. A. Anderson, T. A. Gisby, T. G. McKay, B. M. O'Brien and E. P. Calius, *Journal of Applied Physics* 112, 041101 (2012).
6. R. Pelrine, R. Kornbluh, Q. Pei and J. Joseph, *Science* 287 (5454), 836-839 (2000).
7. R. Pelrine, R. Kornbluh and J. Joseph, *Sensors and Actuators A: Physical* 64 (1), 77-85 (1998).
8. W. Voigt, *Annalen der Physik* 274 (12), 573-587 (1889).
9. A. Reuss, *ZAMM - Journal of Applied Mathematics and Mechanics* 9 (1), 49-58 (1929).
10. F. M. Weiss, X. Zhao, P. Thalmann, H. Deyhle, P. Urwyler, G. Kovacs and B. Müller, "Measuring the bending of asymmetric planar EAP structures," in *Electroactive Polymer Actuators and Devices (EAPAD)*, Proceedings of SPIE 8687 (2013), 86871X-86871X-6.
11. F. M. Weiss, T. Töpfer, B. Osmani, C. Winterhalter and B. Müller, "Impact of electrode preparation on the bending of asymmetric planar electro-active polymer microstructures," in *Electroactive Polymer Actuators and Devices (EAPAD)*, Proceedings of SPIE 9056 (2014) 905607.
12. N. Bowden, S. Brittain, A. G. Evans, J. W. Hutchinson and G. M. Whitesides, *Nature* 393, pp. 146-149 (1998).
13. A. L. Volynskii, S. Bazhenov, O. V. Lebedeva and N. F. Bakeev, *Journal of Materials Science* 35, 547-554 (2000).
14. J. Nohava, N. X. Randall and N. Conté, *Journal of Materials Research* 24 (3), pp. 873-882 (2009).
15. S. Rosset and H. Shea, *Applied Physics A* 110 (2), 281-307 (2013).
16. X. Chen and J. W. Hutchinson, *Journal of Applied Mechanics* 71, 597-603 (2004).